Multiparameter Radar Study of Rainfall: Potential Application to Area–Time Integral Studies

R. RAGHAVAN

Institute for Global Change Research and Education, NASA/Marshall Space Flight Center, Huntsville, Alabama*

V. CHANDRASEKAR

Colorado State University, Fort Collins, Colorado

(Manuscript received 17 August 1993, in final form 30 April 1994)

ABSTRACT

Multiparameter radars measure one or more additional parameters in addition to the conventional reflectivity factor. The combination of radar observations from a multiparameter radar is used to study the time evolution of rainstorms. A technique is presented to self-consistently compare the area–time integral (ATI) and rainfall volume estimates from convective storms, using two different measurements from a multiparameter radar. Rainfall volumes for the lifetime of individual storms are computed using the reflectivity at S band (10-cm wavelength) as well as one-way specific attenuation at X band (3-cm wavelength). Area–time integrals are computed by summing all areas in each radar snapshot having reflectivities (S band) in excess of a preselected threshold. The multiparameter radar data used in this study were acquired by the NCAR CP-2 radar during the Cooperative Huntsville Meteorological Experiment (COHMEX) and the Convection and Precipitation/Electrification Experiment (CaPE), respectively. ATI studies were accomplished in this work using multiparameter radar data acquired during the lifetime of six convective events that occurred in the COHMEX radar coverage area. A case study from the COHMEX field campaign (20 July 1986) was selected to depict the various stages in the evolution of a storm over which the ATI and rainfall volume computations were performed using multiparameter radar data. Another case study from the CaPE field campaign (12 August 1991) was used to demonstrate the evolution of a convective cell based on differential reflectivity observations.

1. Introduction

Conventional radars for meteorological measurements radiate and receive waves of a single fixed polarization at one frequency. Linear polarization has been the choice of the majority of such systems. Recently, several research radars have been modified to a multiparameter mode of operation where several parameters in addition to the conventional reflectivity are measured using either polarization or frequency diversity. Among the multiparameter radars, linear dual-polarization radars are becoming increasingly popular due to applications in the fields of precipitation estimation. Observations from multiparameter radars provide insight into the storm evolution process when the various parameters are observed simultaneously in time (Bringi et al. 1993). Conventionally, multiparameter radars have been used for obtaining pointwise estimates of rainfall rate (Bringi et al. 1982). However, multiparameter radars have seldom been used for estimating mean areal rainfall. In this paper, we study the application of multiparameter radar measurements for obtaining mean areal rainfall estimates via the area–time integral (ATI) procedure.

The results of Doneaud et al. (1984) that showed strong correlations between convective rain volumes and its ATI drew attention to using the ATI method for making area-averaged rainfall measurements. Lopez et al. (1989) showed high correlations between ATI in a storm and the corresponding rain volume while examining radar and rain gauge data from the Florida Area Cumulus Experiment (FACE II). Chiu (1988a,b) examined radar data from the Global Atmospheric Research Program (GARP) Tropical Atlantic Experiment (GATE) and reported strong relationships between instantaneous areawide rainfall and fractional area in excess of a preselected threshold, implying that it was possible to accurately measure rainfall over large areas using a single snapshot. Atlas et al. (1990) showed that these results and the success of their techniques (Doneaud et al. 1984; Lopez et al. 1989; Chiu 1988a,b) were based on the existence of a "well-behaved" probability density function of rain rate over the lifetime

* IGCRE is jointly operated by the University of Alabama in Huntsville and the Universities Space Research Association.

Corresponding author address: Dr. Ravi Raghavan, Code ES42, IGCRE-NASA, Marshall Space Flight Center, Huntsville, AL 35812.

of a single storm or from the multiplicity of storms at any one instant. Kedem et al. (1990) using a probabilistic approach explained the high correlation between the area-averaged rain rate and the fractional area in excess of the preselected threshold and studied the robustness of the slope of the linear relation between them by using different rain-rate distributions. They concluded that the choice of the threshold was critical, especially for the low mean rain rates and that the optimal threshold was probably some function of that mean rain rate. Krajewski et al. (1992) used a Monte Carlo simulation approach to investigate the performance of the area-threshold method by addressing the random and systematic biases in the radar rainfall estimation process. Braud et al. (1993) developed a mathematical framework to explain the relation between mean areal rainfall and the fractional rainy area above a preselected threshold. They reported that the high correlation was mostly dependent on the variabilities of both the fractional rainy area above a threshold and the corresponding mean rain intensity within that area.

In the various studies of ATI based on radar data that are available in the literature, the dataset for rainfall volume V and ATI come from the same radar measurement, except for the case when rainfall volume is computed from rain gauge measurements. Multiparameter radars provide the unique ability whereby the ATI and rainfall volume can be computed from two different parameters that are measured by a multiparameter radar.

In this paper, we present a technique where the ATI and rainfall volume are computed using two independent measurements from a multiparameter radar. The independence that is alluded to here is the measurement independence of radar signals where the statistical fluctuations of the radar signals are uncorrelated (Doviak and Zrnić 1984). The ATI is computed by thresholding on the reflectivity field Z, whereas the rainfall volume is obtained from one-way specific attenuation at X band. In addition, we note that the fundamental physical mechanism that relates the radar measurements to the properties of the rain medium is different in the measurement of reflectivity and attenuation. Reflectivity measurements are dependent on the backscatter characteristics of weather targets, whereas attenuation is a forward scatter or propagation measurement. Thus, if we compute rainfall volume from fields such as X-band attenuation, we obtain independent estimates of rainfall volume. These two estimates of the ATI and rainfall volume are subsequently used to evaluate the ATI technique in a self-consistent manner. Again, by the term *self-consistency,* we refer to the feature that both parameters of the multiparameter radar that are used in the computation of rain volume and ATI come from nearly identical measurement resolution volumes. We also study the various stages of evolution of a storm that form the integrand of an ATI evaluation using multiparameter radars. We have used multiparameter radar data collected by the National Center for Atmospheric Research (NCAR) CP-2 radar during two field experiments, namely, the Cooperative Huntsville Meteorological Experiment (COHMEX) and Convection and Precipitation/Electrification Experiment (CaPE), to accomplish the aforementioned objectives.

Our paper is organized as follows: section 2 describes the procedures used to obtain rainfall estimates using multiparameter radar measurements such as reflectivity Z, differential reflectivity Z_{DR}, specific differential propagation phase K_{DP} at S band (10-cm wavelength), and one-way specific attenuation A_x at X band (3-cm wavelength). In section 3, we outline the procedure used to evaluate the ATI obtained from multiparameter radar measurements. In section 4, we discuss the significance of the multiparameter radar signatures obtained at various stages in the evolution of a storm, accompanied by a brief description of the storm events that were analyzed in this study. Also discussed here are the ATI and rainfall volume estimates obtained using the procedure outlined in section 3. Section 5 summarizes the key results of this paper.

2. Multiparameter radar estimates of rainfall

Application of multiparameter radar techniques to the remote measurement of rainfall rate R has been studied by many scientists (e.g., Aydin et al. 1987; Sachidananda and Zrnić 1986; Chandrasekar et al. 1990). Past studies show that differential reflectivity Z_{DR} can be used with reflectivity Z to estimate rainfall rate in the form (Chandrasekar and Bringi 1988)

$$R_{DR} = C_1 Z^{\alpha} Z_{DR}^{\beta}, \tag{1}$$

where the constants C_1, α, and β depend on the measurement frequency. In Eq. (1), R_{DR} has units of millimeters per hour when Z has its standard units ($mm^6\ m^{-3}$) and Z_{DR} is in decibels. Similarly, estimates of rainfall rate can be obtained from specific differential propagation phase K_{DP} as (Chandrasekar et al. 1990)

$$R_{DP} = C_2 K_{DP}^{\gamma}, \tag{2}$$

where the constants C_2 and γ are functions of the measurement frequency. In Eq. (2), R_{DP} has units of millimeters per hour when K_{DP} is in degrees per kilometer. The one-way specific attenuation A_x at X band can also be used as a measure of rainfall rate in the form

$$R_A = C_3 A_x. \tag{3}$$

Note that there is no exponent on A_x in Eq. (3) and this is a good approximation for relating A_x and R (Bringi et al. 1990). In Eq. (3), R_A has units of millimeters per hour when A_x is in decibels per kilometer. Here K_{DP} and A_x are derived as range derivatives of differential propagation phase ϕ_{DP} and cumulative attenuation CA. The measurement techniques for ob-

taining CA from dual-frequency radar systems has been described in Tuttle and Rinehart (1983). The measurements of ϕ_{DP} and CA come out naturally as range cumulative quantities of K_{DP} and A_x, which have a near-linear relation to rainfall. This feature is very useful, especially in the context of ATI, since the difference in ϕ_{DP} between two range locations r_1 and r_2 is already available as an integral; that is,

$$\phi_{DP}(r_1; r_2) = \int_{r_2}^{r_1} K_{DP}(r)dr. \quad (4)$$

Thus an areal sweep of ϕ_{DP} over regions of rainfall automatically performs the spatial integral of rain rate. This integral can be easily accumulated in time to obtain rainfall volume. Similar arguments are valid for CA also.

3. Multiparameter radar computations of rainfall volume and ATI

The ATI technique of estimating rainfall volume is defined as follows: let $R(a, t)$ be the instantaneous space and time function of rainfall rate. The rainfall volume V can be expressed as

$$V = \int_T \int_{A(t)} R(a, t)dadt, \quad (5)$$

where da and dt are the incremental elements of area and time, respectively; the integration is performed over the regions of area $A(t)$ where the rainfall exceeds a prescribed threshold. The ATI for a storm can be defined as

$$\text{ATI} = \int_T A(t)dt, \quad (6)$$

where the integral in Eq. (6) is typically computed with some threshold on rainfall rate or reflectivity. Using the mean value theorem, V and ATI can be related as

$$V = R_c \text{ ATI}, \quad (7)$$

where R_c is the ATI coefficient relating V and ATI (Doneaud et al. 1984; Lopez et al. 1989; Atlas et al. 1990). The value of R_c depends critically on the threshold used to compute ATI. The utilization of the mean value theorem necessitates computation of the ATI over the full natural distribution of rainfall. Several radar-based assessments of the ATI technique in the past have used the same radar reflectivity measurement to compute rainfall volume V (via a Z–R relation) as well as ATI. A specific rainfall rate can come from many different values of Z and vice versa. Thus when we attempt to integrate over the natural distribution of rainfall to compute V and ATI, the bivariate behavior between them is suppressed. This paper presents independent computations of V and ATI based on multiparameter radar measurements obtained from the same measurement resolution volume for a self-consistent study of the ATI technique.

Our evaluation procedure is as follows. The integral in Eq. (6) can be computed in several ways. In our work, the ATI is computed by summing all areas of radar echoes with reflectivity values greater than the threshold $\text{dB}Z_T$. The ATI integration can be written as

$$\text{ATI} = \sum_{i=1}^{n} A_i \Delta t_i, \quad (8)$$

where A_i is the area comprising reflectivities above the threshold $\text{dB}Z_T$ at the ith radar snapshot of the storm and Δt_i is the time interval between snapshots. The index i on Δt_i indicates the time interval between radar snapshots need not be the same. The time interval between radar pictures has to be small enough to ensure convergence of the summation in Eq. (8) that approximates an integral. The rainfall volume is computed as follows: in each radar beam, ϕ_{DP} or CA at the far end of the storm is the integral of K_{DP} or A_x for the entire beam. However, in practice, we need to subtract the radar system ϕ_{DP} from the range profile of differential propagation phase in order to compute the ϕ_{DP} through the precipitation medium only (Hubbert et al. 1993). Similarly, the difference between the radar system constants at S and X bands have to be subtracted from the observed CA profiles (Tuttle and Rinehart 1983). This ϕ_{DP} or cumulative attenuation is integrated over azimuth to obtain an areal integral of K_{DP} or A_x. These integrals are then transformed to rainfall volumes by using Eqs. (2) and (3). In practice, K_{DP} or A_x is derived at each radar range bin from the estimated ϕ_{DP} or CA profile, respectively. The rainfall rate at any range bin can then be calculated using Eqs. (2) and (3). In this study, we have used Eq. (3) with the constant C_3 equal to 40 to compute rainfall volume based on A_x estimates. This coefficient was obtained using a regression to fit rainfall rate and attenuation from the simulation of various raindrop size distributions (Chandrasekar and Bringi 1988). In addition, we can also compute rainfall volume using a Z–R relationship or using Z and Z_{DR} as in Eq. (1) and then perform a space–time integral. Thus the rainfall volume estimates obtained by one of the above procedures and the ATI are plotted against each other to evaluate the ATI coefficient.

4. Data analysis

We have utilized the multiparameter radar data collected by the CP-2 radar during the COHMEX and CaPE. A more detailed description of COHMEX and CaPE can be found in Dodge et al. (1986) and Foote (1991), respectively. The operational specifications of the CP-2 radar can be found in Bringi and Hendry (1990). The CP-2 radar has a matched beamwidth of

0.94° at S band and X band. Typically, the range resolution at both frequencies is 200 m, and at each radar resolution volume 128 samples of the radar echo returns spaced 1 ms apart (pulse repetition time) were processed. During COHMEX and CaPE, the CP-2 radar operated in the dual-frequency mode, measuring reflectivities at S band (at both H and V polarizations) and X band; one-way specific X-band attenuation (A_x) estimates were obtained from the X-band reflectivity measurements (Tuttle and Rinehart 1983). We have analyzed radar data obtained from six storm cells, following them through their life cycle, to obtain the rainfall volume and ATI estimates for each cell. We also present detailed multiparameter radar signatures through the life cycle of one of the storms (20 July 1986) to demonstrate the various stages of cell evolution. A similar study is done based on Z_{DR} observations for a multicell event (12 August 1991) from the CaPE field campaign.

During COHMEX and CaPE, the radar performed volume sector scans [plan position indicator (PPI) mode] on the storm cells of interest. The cells were observed by radar, from their early evolution until maturity (or steady state), with an approximate 2–3-min interval between scans. This enabled the recording of small-scale microphysical changes, as the cells cycled through from formation to maturity. Subsequent processing of the radar data was done (Mohr and Miller 1983) to yield constant-altitude PPIs (CAPPIs) at 1 km. Vertical cross-sectional profiles of the multiparameter radar observables through the storm cells were obtained in a similar manner. The CAPPIs had a horizontal grid resolution of 500 m. Rainfall volume and ATI estimates for each cell were obtained from these 1-km CAPPIs.

a. Description of storm cells analyzed

1) 19 JULY 1986

Two microburst events were recorded on 19 July, within a half-hour period—the first occurred at 1754 CDT and the second followed at 1820 CDT (henceforth all times are CDT unless specified). A brief description of the likely scenario of storm evolution leading to the microburst event of 1820 based on the detailed analysis presented by Menon (1989) is as follows: the cell was in its early stages of development when it was first detected by CP-2 at 1744. The analysis by Menon (1989) indicated that the storm cell initially evolved via the "warm rain" process (Caylor and Illingworth 1987). Figure 1a shows a CAPPI (at 1-km altitude) at 1756. This CAPPI exhibits a peak reflectivity of 47.5 dBZ; the 30-dBZ contour includes regions of high Z_{DR} (>3 dB). The storm experienced rapid growth between 1808 and 1814. Figure 1b shows a CAPPI (at 1-km altitude) at 1814; peak reflectivity is 56.3 dBZ; the 50-dBZ contour encloses regions of Z_{DR} values greater than 4 dB. The vertical cross-sectional

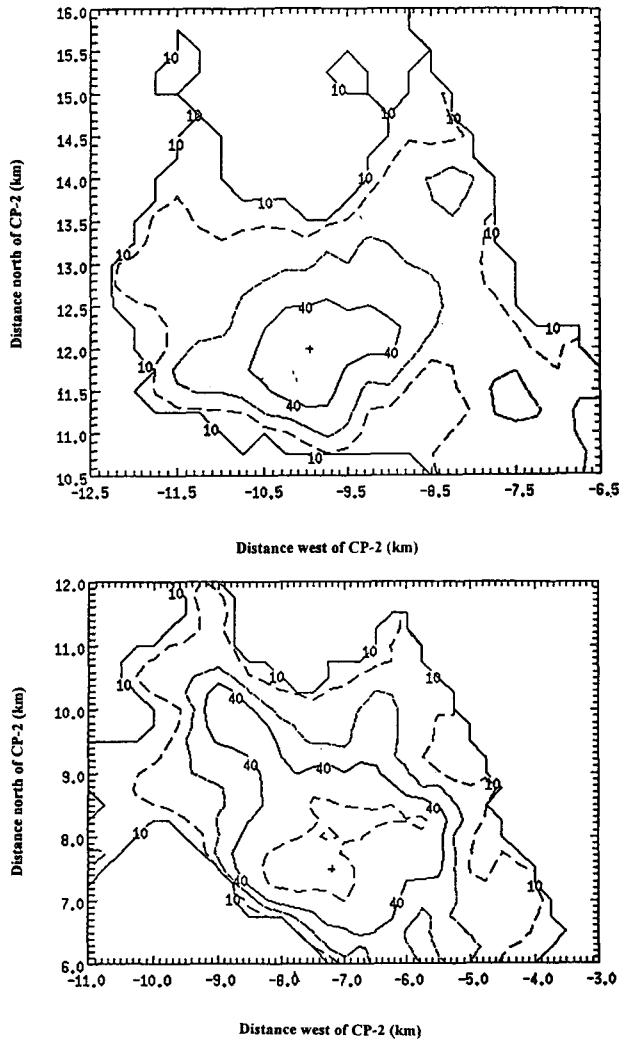

FIG. 1. (a) Horizontal profile (CAPPI at 1 km) of S-band reflectivity Z for the 19 July 1986 storm, at time 1756 CDT. CP-2 located at (0, 0). Horizontal axis represents horizontal distance in kilometers west of CP-2, and vertical axis represents horizontal distance in kilometers north of CP-2. Contours of Z start at 10 dBZ and increment by 10 dB. Peak Z is 47.5 dBZ. (b) Same as (a) except at 1814 CDT and peak Z is 56.3 dBZ.

profiles of Z_{DR} during this time period indicated the presence of a positive Z_{DR} column (values greater than 1 dB) that extended to 6 km in height. The A_x profiles displayed a steady increase in peak values aloft (5.5–6 km in height), from 1.3 dB km^{-1} at 1802 to 2.1 dB km^{-1} at 1814, "indicating accumulation of mixed phase precipitation" at these heights. Profiles of Z, Z_{DR}, and A_x after 1814 indicated an increase in mass content aloft. The analysis by Menon (1989) further indicated that the precipitation core began its descent to the surface when the updraft weakened, which led to the inference that "subsequent mass loading initiated the downdraft whose intensity intensified due to the additional cooling caused by the descending frozen pre-

cipitation while traversing the melting level," and reported that the microburst and the precipitation core arrived simultaneously at the surface.

2) 22 JULY 1986

On 22 July, the CP-2 radar monitored a multicellular storm system located 60–80 km south of the radar, between 1512 and 1611 CDT. In this study, we focus our attention on three cells within this multicellular system, identified as "north cell, south cell, and far south cell." A comprehensive study of this multicell storm can be found in Bringi et al. (1991a). CAPPIs at 1-km altitude were obtained for each radar volume scan between 1512–1611. Multiparameter radar measurements were obtained on the north cell, during its evolution from 1512 to 1605 CDT. Figure 2a shows a CAPPI (at 1 km) for the north cell at 1512, at which time the cell exhibited a well-defined region of reflectivities greater than 40 dBZ. Figure 2b shows a CAPPI (at 1 km) for the north cell at 1531, where it is evident that the cell has grown in areal extent, exhibiting two distinct regions of reflectivities greater than 40 dBZ. Between 1543 and 1557, the CAPPIs (at 1 km) indicated that the north cell had peak reflectivities of 54 dBZ. The analysis of Bringi et al. (1991a) indicated that between 1553 and 1605, the cell was in a downdraft phase that resulted in a further reduction of reflectivity values.

The south cell was tracked by radar from its evolution at approximately 1538 to 1605 after which time it merged with the far south cell. Bringi et al. (1991a) inferred that the south cell was dominated by the "warm rain" process. The south cell experienced rapid growth at 1543. Vertical cross-sectional profiles through the south cell at 1545 showed a positive Z_{DR} column (>3 dB) that extended to 5 km in altitude with a 45-dBZ contour that extended to an altitude of 6.5 km. Here A_x profiles displayed a core of A_x values greater than 2.2 dB km^{-1} centered at an altitude of 4.8 km. Cross-sectional profiles of Z_{DR} at 1548 indicated that glaciation had occurred; the descent of the precipitation core was evident in the 1557 profiles. The CAPPI (at 1 km) at 1557 displayed a peak reflectivity of 52.9 dBZ and values of $A_x > 1.0$ dB km^{-1}.

The far south cell was detected at 1543 and its evolution was tracked by radar until 1611. At 1557, the CAPPI (at 1 km) indicated that the cell had a well-defined region of reflectivities greater than 40 dBZ; the 40-dBZ contour enclosed regions of Z_{DR} values greater than 1.5 dB and $A_x > 0.5$ dB km^{-1}. We refer to Bringi et al. (1991a), wherein the cross-sectional profile through the far south cell at 1557 shows a peak Z of 54.4 dBZ at an altitude of 4.4 km with a peak Z_{DR} of 4.6 dB at an altitude of 3.6 km. Their analysis led to the inference that "this cell was forced by low-level convergence produced by the interaction of the outflow boundary (generated by a storm complex located 85–90 km south of the radar) with low-level outflow from the south (or north cell)."

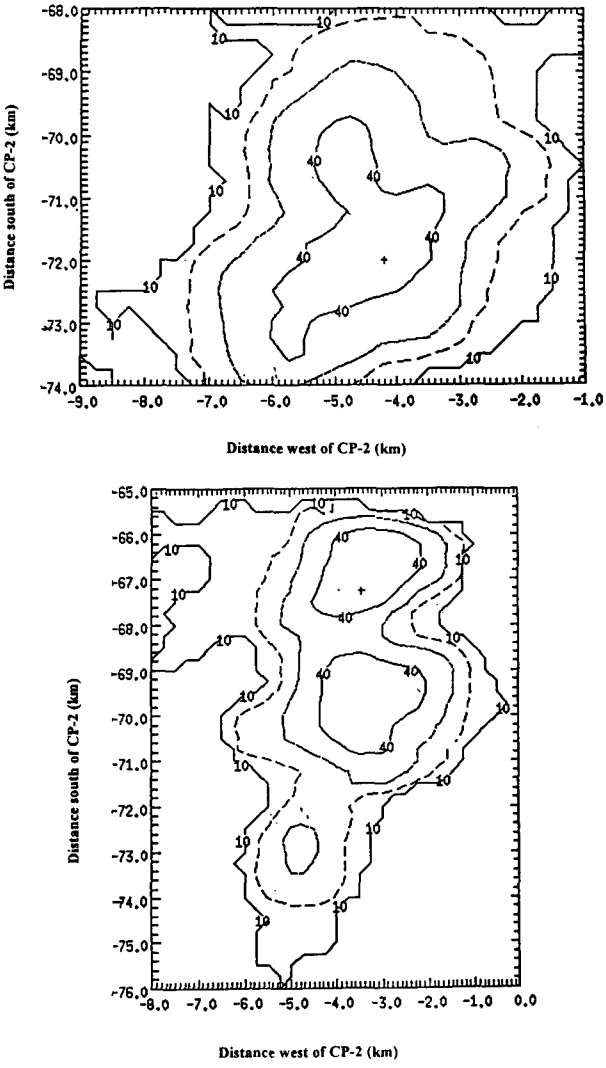

FIG. 2. (a) Horizontal profile (CAPPI at 1 km) of S-band reflectivity Z for the 22 July 1986 storm, at time 1512 CDT. CP-2 located at (0, 0). Horizontal axis represents horizontal distance in kilometers west of CP-2, and vertical axis represents horizontal distance in kilometers south of CP-2. Contours of Z start at 10 dBZ and increment by 10 dB. Peak Z is 43.8 dBZ. (b) Same as (a) except at time 1531 CDT and peak Z is 48.1 dBZ.

3) 24 JULY 1986

On 24 July, the radar tracked a microburst-producing storm from its early stage of evolution at 1343 to its collapse at 1407 CDT. Bringi et al. (1991b) provide a detailed microphysical study of this cell, wherein they conclude that "this cell was formed below the anvil region and along the outflow boundary of a multicell system, located 55 km south of the CP-2 radar." Their analysis indicated that the cell was initiated via a warm

rain process. The cell experienced rapid vertical growth from 1351 to 1356. At 1356, peak Z was 66 dBZ at 6.5-km altitude. At 1359, a region of high attenuation values extended from 3 to 5 km in altitude. At 1401, the descent of the precipitation core was evident in the radar cross-sectional profiles, with a peak Z of 61 dBZ at 5-km height. The CAPPI (at 1 km) at 1401 displayed regions of $A_x > 1.5$ dB km^{-1}.

b. *Time evolution studies of the 20 July 1986 storm*

On 20 July, CP-2 observed an isolated storm that developed in the COHMEX radar coverage area. Tuttle et al. (1989) state that "this storm subsequently produced heavy rain, small hail, and a microburst at the surface"; a detailed analysis of this microburst event and the environmental conditions on that day can be found therein. For this study, the multiparameter radar data from the rain layer of this storm were averaged to obtain profiles of Z_{DR} and A_x with respect to time. Figures 3a–d show time sequence of the Z_{DR} versus reflectivity in the rain layer; each point in this profile represents the average Z_{DR} for each 2-dB increment in Z. Figures 3a–d correspond to times 1402, 1414, 1420, and 1436 CDT (all the time profiles are not shown here for brevity). In these figures, Z ranges from 10 to 60 dBZ. For a given Z, the feature of reducing Z_{DR} with time implies that the raindrop spectrum is changing from one dominated by a lower concentration of large raindrops to one dominated by a higher concentration of smaller raindrops. The spectrum eventually seems to attain some sort of equilibrium, seen by a steady relationship between Z and Z_{DR}. Figures 4a–d show similar profiles of specific attenuation A_x at 1402, 1414, 1424, and 1432 CDT. Unlike Z_{DR}, which is a relative measurement related to the median drop size, A_x is proportional to the rainfall rate in the rain layer. Thus, Figs. 4a–d demonstrate the evolution of rainfall produced by the storm. This unique observation is possible from the use of multiparameter radar data. The range of specific attenuation A_x varies from 0.1 to 7 dB km^{-1}. In the early stages of the storm the attenuation is small indicating low rain rates. However, by 1415 the attenuation increases rapidly for reflectivities greater than 50 dBZ ($A_x > 1$ dB km^{-1}), indicating intense rain. On the dissipating stages of the same storm, the attenuation again decreases rapidly indicating low and steady rain rates. We note, however, that such features cannot be observed with reflectivity alone based on a Z–R relationship, since all the same reflectivities would have been associated with the same rainfall rates. We also note that the time profiles of attenuation are different from those of Z_{DR}; the profiles of Z_{DR} show primarily the nature of the raindrop spectral evolution. The time profiles of specific attenuation also delineate the rainfall at various stages of the storm evolution that are considered for rainfall volume estimates in the ATI procedure.

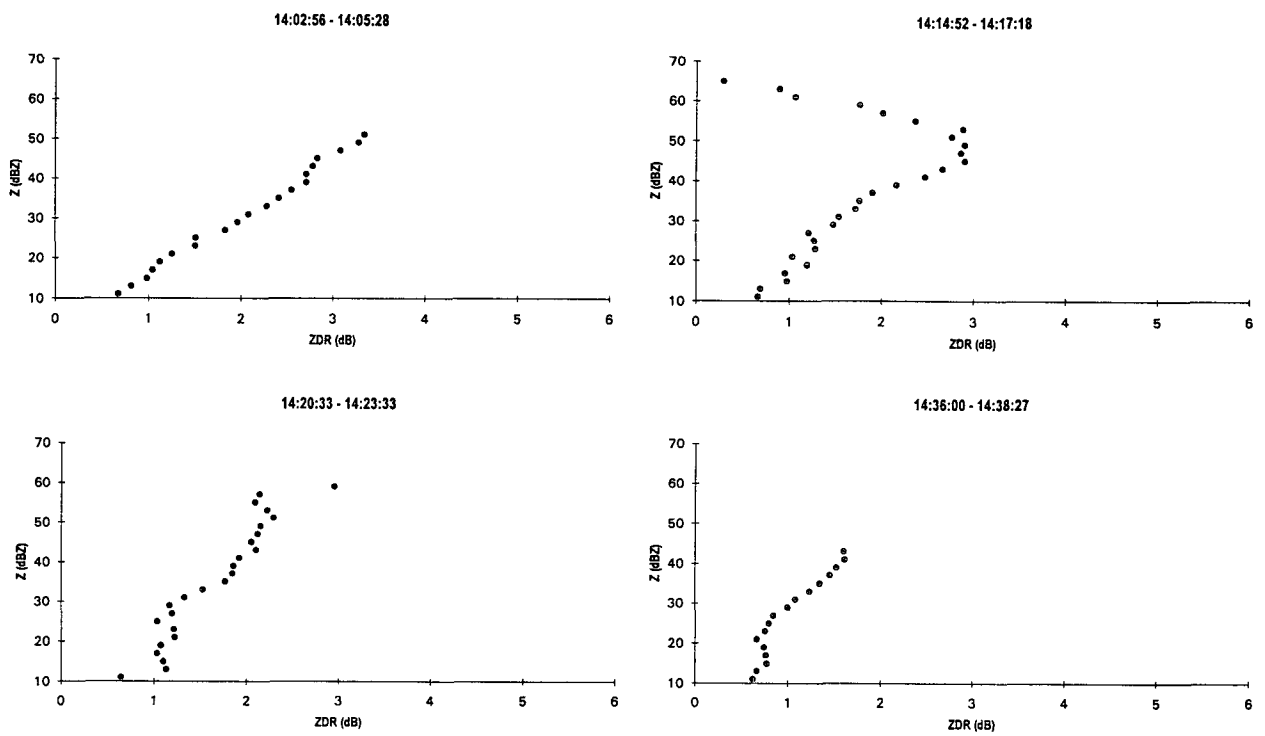

FIG. 3. (a)–(d) Time sequence of average Z_{DR} for each 2-dB increment in Z versus reflectivity in the rain layer for the 20 July 1986 storm.

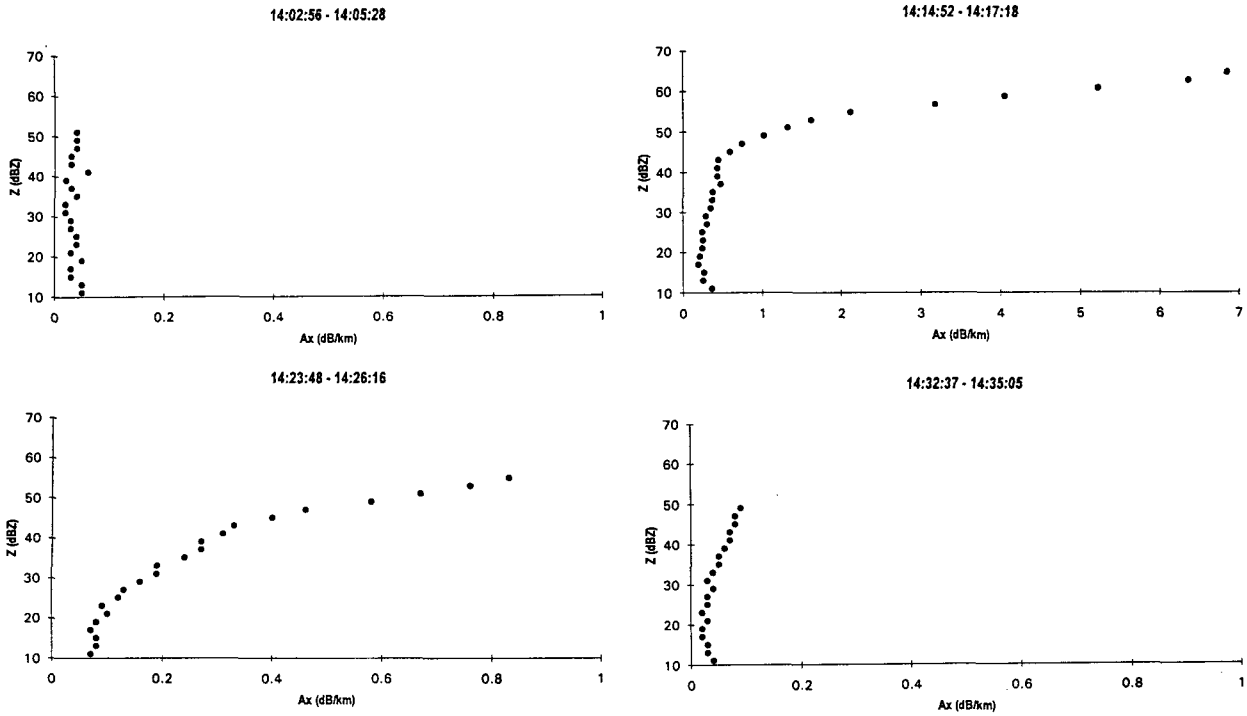

FIG. 4. (a)–(d) Time sequence of average A_x for each 2-dB increment in Z versus reflectivity in the rain layer for the 20 July 1986 storm.

c. *Time evolution studies of the 12 August 1991 storm based on Z_{DR} observations*

In this section, we examine the evolution of a storm from the CaPE field program using differential reflectivity observations. The volume median drop diameter D_o is a function of rainfall rate (Marshall and Palmer 1948) and can be derived from the magnitude of the Z_{DR} observations in rain (Illingworth and Caylor 1989). The time-sequence histogram of D_o over a duration spanning the evolution of the storm can provide insight into the various integrands in the ATI calculation over the life cycle of a storm. The storm under consideration is a multicell event observed by the CP-2 radar on 12 August 1991 between 2205 and 2227 UTC. A detailed analysis of the radar observations from this event can be found in Goodman and Raghavan (1993). Their analysis indicated that the storm experienced renewed growth between 2209 and 2218 UTC and sustained vertical growth between 2218 and 2227 UTC with reflectivities greater than 50 dBZ extending to a height of 10 km; cloud tops reached 16 km at 2227 UTC. Figure 5 shows the profiles of maximum reflectivity as a function of height, for the six volume scans performed by the radar between 2205 and 2227 UTC (Goodman and Raghavan 1993). It is evident in this figure that the maximum Z does not change much below the melting level (4.5 km), although there is dramatic vertical development in Z aloft at 2209 and 2227 UTC. Figures 6a–e show the volume median drop diameter D_o histograms for the six volume scans. The D_o histograms were derived from Z_{DR} observations (Illingworth and Caylor 1989) that were obtained from CAPPIs at 0.5-km altitude. Between 2209 and 2218 UTC, the histograms exhibit broad distributions, indicating that the storm is in the growth phase. Between

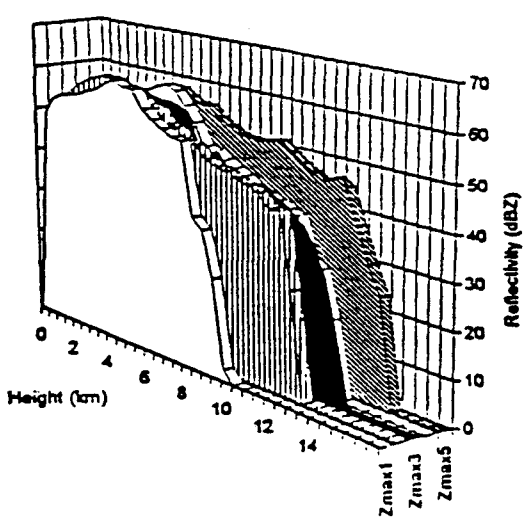

FIG. 5. Time–height evolution of the vertical profile of maximum S-band radar reflectivity Z for the 12 August 1991 storm; Zmax1, Zmax3, and Zmax5 correspond to the radar volume scans at 2205, 2213, and 2227 UTC. (Adapted from Goodman and Raghavan 1993.)

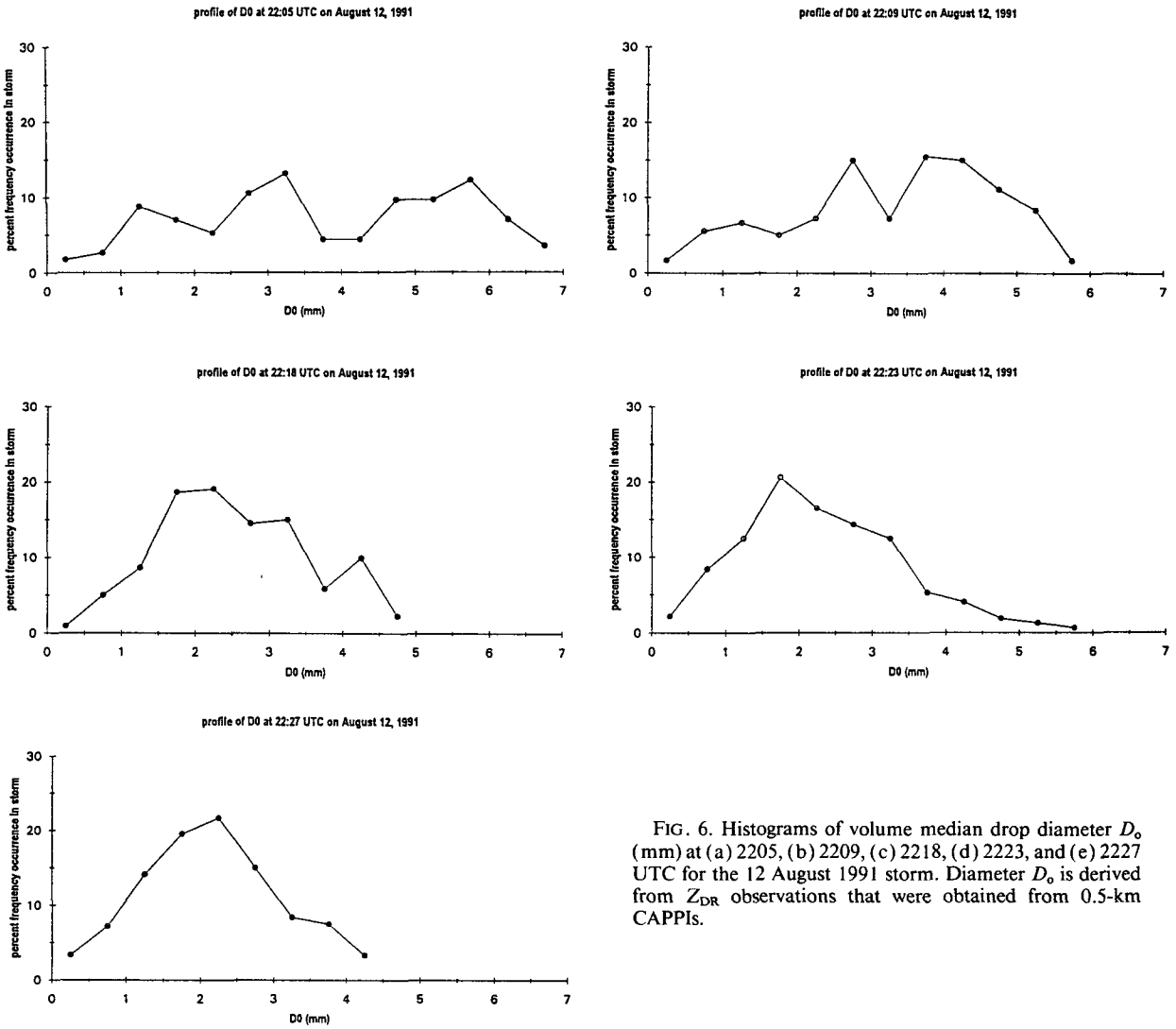

FIG. 6. Histograms of volume median drop diameter D_0 (mm) at (a) 2205, (b) 2209, (c) 2218, (d) 2223, and (e) 2227 UTC for the 12 August 1991 storm. Diameter D_0 is derived from Z_{DR} observations that were obtained from 0.5-km CAPPIs.

2223 and 2227 UTC, the D_o histograms show more narrow distributions indicating lower concentrations of the larger sized drops. The evolution of D_o relates to the evolution of rainfall as observed by the radar.

d. ATI analysis

Multiparameter data acquired by the NCAR CP-2 radar through the lifetime of six convective storms (discussed in sections 4a and 4b) during the COHMEX field campaign were used for performing the ATI analysis. We do not include multiparameter radar data acquired from the CaPE field campaign for the ATI analysis, because the radar did not observe the full evolution of the storm (discussed in section 4c). The rainfall volume for the lifetime of each individual storm is obtained from the one-way specific attenuation A_x at X band using Eq. (3). The ATI is computed from elemental areas having reflectivities in excess of a preselected threshold using Eq. (8). Figure 7 shows a plot of rainfall volume obtained from A_x and the ATI computed using a 25-dBZ reflectivity threshold for the six storms used in this study. Similar results are shown in Fig. 8, where the rainfall volume has been obtained using the Marshall–Palmer (1948) Z–R relationship. The ATI coefficient estimated from Fig. 7 is 12.87, whereas the ATI coefficient estimated from Fig. 8 is 14.30. The ATI calculations were similarly performed using reflectivity thresholds of 20 and 30 dBZ. The ATI coefficients obtained from the regression between rainfall volume and ATI for the three different reflectivity thresholds are shown in Table 1. The ATI coefficient increases with the reflectivity threshold, which is in agreement with the theoretical findings of Atlas et al. (1990). We note here that the rainfall volume and ATI estimates are obtained from independent radar measurements for the results of Fig. 7 due to the measurement procedure. We have not included the V–ATI regression correlation coefficients in Table 1, as they are not meaningful for the small number of data

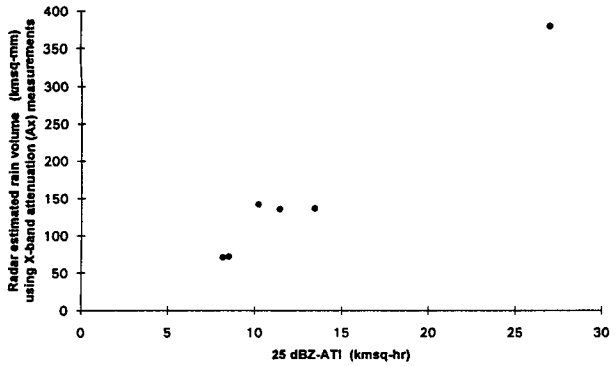

FIG. 7. Scatterplot of the rainfall volumes versus the 25-dBZ area–time integrals for 6 storms from COHMEX. Data collected by the NCAR CP-2 radar. The rainfall volumes have been estimated using one-way specific X-band attenuation A_x.

points that we have used for this study. The ATI coefficient obtained from Fig. 8 is slightly higher than that from Fig. 7 and can probably be adjusted by using a different Z–R relationship.

5. Summary and conclusions

Conventionally, multiparameter radar observations of rainfall have been used to obtain instantaneous point estimates of rainfall. In this paper, we have used multiparameter radar data for applications involving mean areal precipitation. Multiparameter radars provide the unique advantage of observing the spatial and temporal distribution of the precipitation microphysics that is included in the averaging process. We have presented a technique to compute storm rainfall volume and the corresponding ATI using multiparameter radar measurements in a self-consistent way. Multiparameter radar data were acquired by the NCAR CP-2 radar during the COHMEX and CaPE field campaigns conducted in Alabama and Florida in 1986 and 1991, respectively. In this study, the rainfall volume over the lifetime of individual storms was computed from the one-way

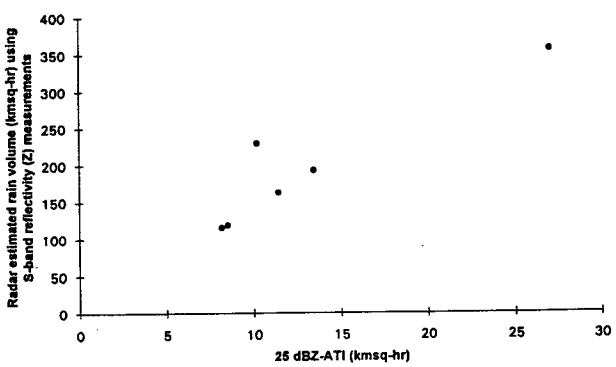

FIG. 8. Same as Fig. 7 except rainfall volumes have been estimated using Marshall–Palmer (1948) Z–R relation.

TABLE 1. ATI coefficients obtained from the regression between rainfall volume and ATI for different reflectivity thresholds. The rainfall volumes are computed based on the A_x and Z–R methods.

Reflectivity threshold used for computing ATI	ATI coefficient based on the A_x method	ATI coefficient based on the Z–R method
20 dBZ	10.89	12.06
25 dBZ	12.87	14.30
30 dBZ	16.20	18.11

specific attenuation at X band (3-cm wavelength) as well as by using the Marshall–Palmer (1948) Z–R relation. The ATI was computed by summing up elemental areas in each radar snapshot, whose reflectivities exceeded a preselected threshold; integration was performed for the duration of the storm. The time interval between successive radar snapshots was 2–3 min. We have applied this procedure to multiparameter radar data acquired from COHMEX and demonstrated its applicability. ATI calculations were done for a range of reflectivity thresholds. The ATI coefficient increased with the reflectivity threshold; this is consistent with the theoretical considerations of Atlas et al. (1990). It is noteworthy that in this study, the rainfall volume and ATI estimates are obtained from two independent measurements from a multiparameter radar; that is, rainfall volume estimates were obtained from one-way specific attenuation at X band, whereas the ATIs were calculated using S-band reflectivity. We recognize that our dataset is small to draw significant conclusions from this preliminary study and realize that an extensive experimental effort is required to assess the V–ATI computations using this procedure. However, our demonstration presents a new way to utilize multiparameter radar data for studies involving mean areal precipitation estimates. We have also depicted the various stages of evolution of a single storm (20 July 1986) and delineate the various stages of the evolution of a cell that are included in the rainfall volume and mean areal precipitation estimation process.

Acknowledgments. This research was supported by NASA through USRA subcontract SUB93-216 under NASA Cooperative Agreement NCC8-22 and CSU subcontract. The authors also acknowledge the useful discussions with Prof. V. N. Bringi at Colorado State University and Dr. S. J. Goodman at NASA/Marshall Space Flight Center.

REFERENCES

Atlas, D., D. Rosenfeld, and D. Short, 1990: The estimation of convective rainfall by area integrals, 1. The theoretical and empirical basis. *J. Geophys. Res.*, **95**, 2153–2160.

Aydin, K., H. Direskeneli, and T. A. Seliga, 1987: Dual-polarization radar estimation of rainfall parameters compared with ground-based disdrometer measurements, October 29, 1982, Central Illinois Experiment. *IEEE Trans. Geosci. Remote Sens.*, **25**, 834–844.

Braud, I., J. D. Creutin, and C. Barancourt, 1993: The relation between the mean areal rainfall and the fractional area where it rains above a given threshold. *J. Appl. Meteor.*, **32,** 193–202.

Bringi, V. N., and A. Hendry, 1990: Technology of polarization diversity radars for meteorology. *Radar in Meteorology,* D. Atlas, Ed., Amer. Meteor. Soc., 153–190.

——, T. A. Seliga, and E. A. Mueller, 1982: First comparisons of rainfall rates derived from radar differential reflectivity and disdrometer measurements. *IEEE Trans. Geosci. Remote Sens.*, **20,** 202–204.

——, V. Chandrasekar, N. Balakrishnan, and D. S. Zrnić, 1990: An examination of propagation effects in rainfall on radar measurements at microwave frequencies. *J. Atmos. Oceanic Technol.*, **7,** 829–840.

——, D. A. Burrows, and S. M. Menon, 1991a: Multiparameter radar and aircraft study of raindrop spectral evolution in warm-based clouds. *J. Appl. Meteor.*, **30,** 853–880.

——, D. A. Burrows, and J. Vivekanandan, 1991b: Multiparameter radar and aircraft study of raindrop spectral evolution in warm-based clouds. Preprints, *25th Int. Radar Conf. on Radar Meteorology,* Paris, France, Amer. Meteor. Soc., 708–712.

——, A. Detwiler, V. Chandrasekar, P. L. Smith, L. Liu, I. J. Caylor, and D. Musil, 1993: Multiparameter radar and aircraft study of the transition from early to mature storm during CaPE: The case of 9 August 1991. Preprints, *26th Int. Conf. on Radar Meteorology,* Norman, OK, Amer. Meteor. Soc., 318–320.

Caylor, I. J., and A. J. Illingworth, 1987: Radar observations and modeling of warm rain initiation. *Quart. J. Roy. Meteor. Soc.*, **113,** 1171–1191.

Chandrasekar, V., and V. N. Bringi, 1988: Error structure of multiparameter radar and surface measurements of rainfall. Part I: Differential reflectivity. *J. Atmos. Oceanic Technol.*, **5,** 783–795.

——, ——, N. Balakrishnan, and D. S. Zrnić, 1990: Error structure of multiparameter radar and surface measurements of rainfall. Part III: Specific differential phase. *J. Atmos. Oceanic Technol.*, **7,** 621–629.

Chiu, L. S., 1988a: Estimating areal rainfall from rain area. *Tropical Rainfall Measurements,* J. S. Theon and N. Fugono, Eds., A. Deepak, 361–367.

——, 1988b: Rain estimation from satellites: Areal rainfall-rain area relation. Preprints, *Third Conf. on Satellite Meteorology and Oceanography,* Anaheim, CA, Amer. Meteor. Soc., 363–368.

Dodge, J., J. Arnold, G. Wilson, J. Evans, and T. T. Fujita, 1986: The Cooperative Huntsville Meteorological Experiment (COHMEX). *Bull. Amer. Meteor. Soc.*, **67,** 417–419.

Doneaud, A. A., S. I. Niscov, D. L. Prignitz, and P. L. Smith, 1984: The area–time integral as an indicator for convective rainfall volumes. *J. Climate Appl. Meteor.*, **23,** 555–561.

Doviak, R. J., and D. S. Zrnić, 1984: *Doppler Radar and Weather Observations.* Academic Press, 458 pp.

Foote, G. B., 1991: Scientific overview and operations plan for the CaPE. NCAR, 136 pp.

Goodman, S. J., and R. Raghavan, 1993: Investigating the relation between precipitation and lightning using polarimetric radar observations. Preprints, *26th Int. Conf. on Radar Meteorology,* Norman, OK, Amer. Meteor. Soc., 793–795.

Hubbert, J., V. Chandrasekar, V. N. Bringi, and P. Meischner, 1993: Processing and interpretation of coherent dual-polarized radar measurements. *J. Atmos. Oceanic Technol.*, **10,** 156–164.

Illingworth, A. J., and I. J. Caylor, 1989: Polarization radar estimates of raindrop size spectra and rainfall estimates. *J. Atmos. Oceanic Technol.*, **6,** 939–949.

Kedem, B., L. S. Chiu, and Z. Karni, 1990: An analysis of the threshold method for measuring area-average rainfall. *J. Appl. Meteor.*, **29,** 3–20.

Krajewski, W. F., M. Morrissey, J. A. Smith, and D. T. Rexroth, 1992: The accuracy of the area threshold method—A model-based simulation study. *J. Appl. Meteor.*, **31,** 1396–1406.

Lopez, R. E., D. Atlas, D. Rosenfeld, J. Thomas, D. O. Blanchard, and R. L. Holle, 1989: Estimation of rainfall using radar echo area time integral. *J. Appl. Meteor.*, **28,** 1162–1175.

Marshall, J. S., and W. M. K. Palmer, 1948: The distribution of raindrops with size. *J. Appl. Meteor.*, **5,** 165–166.

Menon, S. M., 1989: Multiparameter radar studies of microbursts and nonmicroburst clouds during MIST. M.S. thesis, Colorado State University, 105 pp.

Mohr, C. G., and L. J. Miller, 1983: CEDRIC—A software package for cartesian space editing, synthesis and display of radar files under interactive control. Preprints, *21st Conf. on Radar Meteorology,* Edmonton, Canada, Amer. Meteor. Soc., 569–574.

Sachidananda, K., and D. S. Zrnić, 1986: Differential propagation phaseshift and rainfall rate estimation. *Radio Sci.*, **21,** 235–247.

Tuttle, J. D., and R. E. Rinehart, 1983: Attenuation correction in dual wavelength analyses. *J. Climate Appl. Meteor.*, **22,** 1914–1921.

——, V. N. Bringi, H. D. Orville, and F. J. Kopp, 1989: Multiparameter radar study of a microburst: Comparison with model results. *J. Atmos. Sci.*, **46,** 601–620.